Microwave induced phonons imaging by Brillouin microscopy

B. Vincent, O. Elmazria, L. Le Brizoual, L. Bouvot, D. Rouxel, P. Alnot.
Laboratoire de Physique des Milieux Ionisés et Applications
CNRS-UMR 7040, Université H. Poincaré, Nancy I
Nancy, France
brice.vincent@lpmi.uhp-nancy.fr

J. K. Krüger, M. Kolle
Fachrichtung 7.2, Experimentalphysik,
Universität des Saarlandes;
Sarrebrücken, Germany

***Abstract*—Bulk Acoustic Waves (BAW) as well as Surface Acoustic Waves (SAW) have been studied by Brillouin Spectroscopy (BS). Experiments performed on Lithium Niobate single crystals and Zinc Oxide thin films have pointed out that BS is able to detect piezoelectrically induced phonons. Propagation losses and spatial acoustic field distribution have then been measured. Results are compared with previous ones obtained with other methods.**

Index Terms—*SAW devices, Lithium niobate, Zinc oxide, thin films, Brillouin spectroscopy.*

I. INTRODUCTION

Surface acoustic wave (SAW) devices are based on inter-digital transducers (IDT) electrodes combined with a piezoelectric material [1,2]. Two main ways have been investigated to optimize these components: the electrodes design and the material properties. To provide electrodes enhancement, one have to know the acoustic field distribution. Up to now, several techniques have been used in order to visualise acoustic fields like optical interferometry [3], atomic force microscopy [4], x-ray spectroscopy [5] and scanning electron microscopy [6]. Obviously methods that measure directly acoustic properties would be the most efficient ones and that holds especially true for the GHz range.

In this paper we demonstrate that Micro-Brillouin (μ-BS), which is well known for the characterisation of elastic properties of the material (thermal phonons), can also be applied to the detection of piezoelectrically induced phonons. Moreover, since Brillouin spectroscopy is able to detect signal as weak as thermal excited phonons, this method can be consider as highly sensitive. Two different devices are used : one fabricated on lithium niobate single crystal with aluminium IDTs deposited by sputtering and another one based on ZnO thin film deposited on silicon wafer.

II. EXEPRIMENTAL SET-UP

A. Brillouin spectroscopy

To detect coherently excited phonons, the interaction between phonons and photons must respect the laws of conservation of momentum and energy. The main difficulty consists in varying the wavelength of the detected phonon and simultaneously maintaining the wave vector parallel to the surface of the device (especially for surface waves). RIθA scattering geometry permits to overcome this problem [7]. Indeed, by rotating the sample around the axis N2 (see fig.1) we can change continuously the angle of incidence and then, adjust in a self-controlling manner the magnitude of the detected phonon wave vector without changing the direction of propagation. In addition, RIθA scattering geometry allows to perform our experiment even if we don't know the value of the refractive index of the piezoelectric material [8].

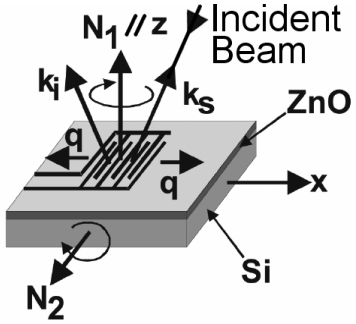

Figure 1 : Schematic view of the RIΘA scattering geometry with IDT deposited on ZnO/Si device. (q is the phonon wavevector, N_1 and N_2 are two axis of rotation, k_i and k_s are respectively the incident and the scattered wavevector of interest, x is the direction of propagation)

Figure 1 describes the RIΘA scattering geometry in the case of ZnO/Si device. In this geometry, the reflected beam is considered as a virtual incident beam, that's why a mirror must coat the device. Anyway, in the special case of ZnO/Si device, silicon wafer can be used as a mirror. For lithium niobate devices aluminium thin film (~ 100 nm) will be deposited on the wafer. The scattered light is collected by the same lens used to focus the incident beam. The Fabry-Perot spectrometer is then used to discriminate the frequencies of the scattered photons. One have to keep in mind that the frequency shift of the photon during the interaction with acoustic phonons is of the order of the GHz instead of Raman

scattering which implies optical phonons with frequency shift of several THz. It explains that a Fabry-Perot interferometer is needed and not only an optical grating. For this "reflection induced scattering geometry" the relation between the sound velocity $V^{\Theta A}$ and the frequency shift read on Brillouin spectrum $f^{\Theta A}$ for a given acoustic wave vector $q^{\Theta A}$ is given by the relation:

$$V^{\Theta A} = \frac{2\pi f^{\Theta A}}{q^{\Theta A}} = f^{\Theta A}.\frac{\lambda_0}{2n_i.\sin\frac{\Theta_i}{2}} = f^{\Theta A}.\frac{\lambda_0}{2.\sin\frac{\Theta}{2}} \qquad (1)$$

Where λ_0 is the wavelength of the laser in vacuum, n_i is the refractive index of the material and Θ is the angle of incidence.

B. *Lithium niobate device preparation*

As a sample we used a commercial (Y+41°)-cut of $LiNbO_3$ (X,Y and Z are the crystallographic axis according to IRE-Standards (1957 and 1961) [9,10]). The plate-like sample with parallelepiped shape is double side optically polished. The z-axis of the rectangular sample coordinate system has been chosen to be orthogonal to the plate surface and co-linear to the (Y+41°)-axis. The thickness is Δz = 300 µm. The crystallographic X-axis has been chosen to be directed along the x-axis of the crystal plate having a length of Δx = 20 mm. The width of the crystal plate is Δy = 15 mm.

The IDT is connected by gold wires to microwave connectors. The spatial period of the IDT is L=14 µm and the total surface of the array is about 1x1 mm^2. The IDT coupled with the acoustic wave velocity defined the frequency of operation at 338 MHz. The generator is electrically decoupled from the sample by a broadband isolator. The standing wave ratio has been measured to be SWR=2.15 which is rather satisfactory. The piezoelectric constant of interest for the excitation of the hypersonic waves is d_{15}=13 pm/V.

C. *ZnO device preparation*

Due to their high electromechanical coupling coefficient ZnO films have been widely investigated as a piezoelectric material for surface acoustic wave (SAW) devices [11-13]. For our application we have sputtered the piezoelectric ZnO film on a silicon substrate that allows the monolithic integration of the acoustic elements and the associated electronic circuit [13]. Zinc oxide films elaborated by sputtering techniques are very sensitive to the deposition parameters: pressure, temperature, gas fraction, the target-substrate distance, etc…[14] The deposition conditions were optimized in order to obtain highly oriented polycrystalline ZnO films. These films were deposited by a DC planar magnetron sputtering system on silicon (100) substrates. The distance between the cathode and the substrate holder was 80 mm. The deposition chamber was pumped down to a base pressure of 5.10^{-7} mbar prior to the introduction of the argon-oxygen gas mixture for the ZnO thin film production. The gas discharge mixture was Ar/O_2 and the total pressure was 2.10^{-3} mbar. For optimum deposition condition, the oxygen percentage in the Ar/O_2 gas mixture was fixed at 70 % and the DC power delivered by the DC generator was fixed to 120 W. The substrate and the chamber wall were grounded and the substrate holder was heated to a temperature of 200°C prior to deposition.

III. RESULTS AND DISCUSSION

A. *Lithium niobate device characterisation*

First of all we have tried to compare the magnitude of induced phonon and thermal phonons. Figure 2 points out the extraordinary amplification of phonons by electric field applied on the IDT. As can be seen, the induced phonons are several orders of magnitude stronger than thermal phonons. One should note that this figure presents results concerning surface waves but similar experiments have been done with bulk waves.

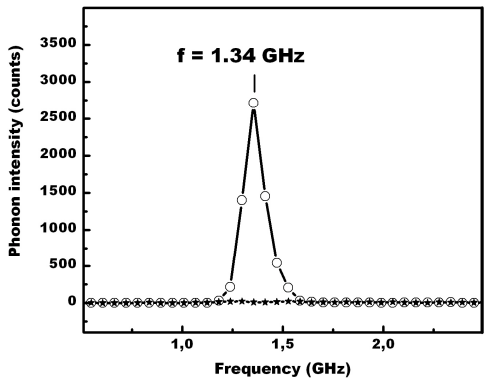

Figure 2 : Comparison between thermal phonons (stars) and piezoelectrically induced phonons (circles)

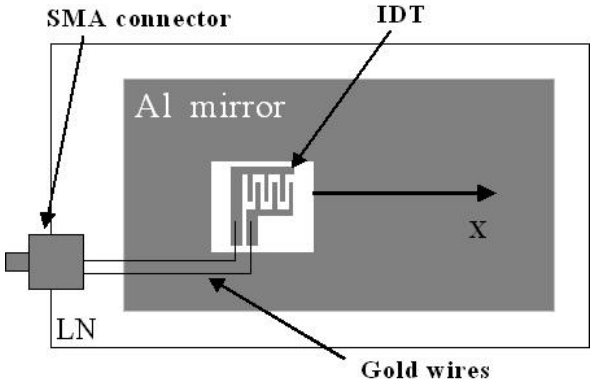

Figure 3 : Schematic view of the lithium niobate SAW device, X indicates the direction of propagation of the induced acoustic wave

The related microwave power applied to the input of the SAW device was 15.9 dBm and the accumulation time of the spectrum was 3 minutes. The thermal phonon line was too small to be clearly detected during this short accumulation

time. The induced phonon line showed a peak intensity of about 2750 counts after an accumulation time of 3 min. Of course the amplitude of the induced phonons is proportional to the electric power applied.

Such amplitudes allow propagation loss measurements.

We have then measured the amplitude of the acoustic wave along the direction of propagation of the beam. Figure 3 presents schematically the device used to realize this measurement. X is the direction of propagation of the induced acoustic wave.

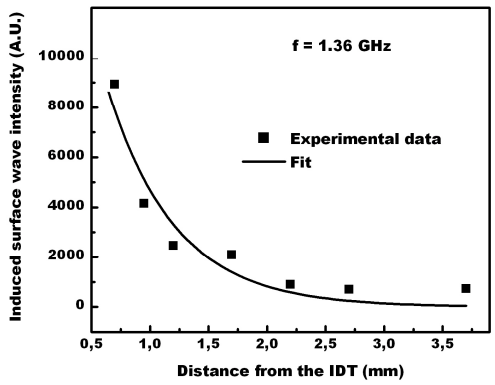

Figure 4 : Induced phonons intensity versus the distance from the IDT. (X direction, see figure 3)

We can observe on figure 4 that the amplitude of the surface acoustic wave decreases exponentially. The fit has been realized by using equation 2:

$$I(x) = I_0 . e^{-\alpha . x} \qquad (2)$$

where I (arbitrary unit) is the integrated phonon intensity, I_0 is the integrated phonon intensity on the border of the IDT (arbitrary unit), x is the distance from the point of analysis to the border of the IDT (mm) and α is the loss (dB/mm).

Several other experiments have been performed for bulk acoustic waves. The results are summarized and compared with previous work in table 1.

TABLE I

PROPAGATION LOSSES MEASUREMENTS (dB/Λ)

References	Surface Waves Attenuation	Bulk Waves Attenuation
Present Work	16.10^{-3}	4.10^{-3}
Hashimoto *et al* [15]	95.10^{-3}	-
Bloch *et al* [16]	14.10^{-3}	-
Grace *et al* [17]	-	5.10^{-5}

As can be seen in table 1, there is a good correlation between propagation losses of surface waves obtained in this study and previously by other authors. However, the discrepancy for bulk waves is of two orders of magnitude. Until now, the reason for the divergence of these values is still unclear but the only uncertainties are not sufficient to explain this phenomenon.

B. ZnO/Si device characterisation

Similar experiments have been done with ZnO/Si devices. As previously mentioned, the silicon wafer used for ZnO deposition also acts as mirror for RIΘA scattering geometry. Then, the first question that arises from this configuration concerns the efficiency of the polished silicon wafer to act as a mirror. Several experiments realised in our group on thermal phonons have pointed out that silicon wafer reflectivity is large enough to obtain efficient Brillouin scattering signal.

Two types of measurements have been realised on this device. First of all propagation losses have been measured for the surface waves. Results obtained for our device is of the order of 200 mm^{-1} which is of course to high and one order of magnitude higher than previous works [18]. Several reasons can explain such losses but mainly the quality of our thin film. Taking into account that the ZnO film is polycrystalline and build up of nano-sized grain, all boundaries grain will increase propagation losses. We have then measured the acoustic wave amplitude perpendicularly to the direction of propagation in order to determine the divergence of the beam.

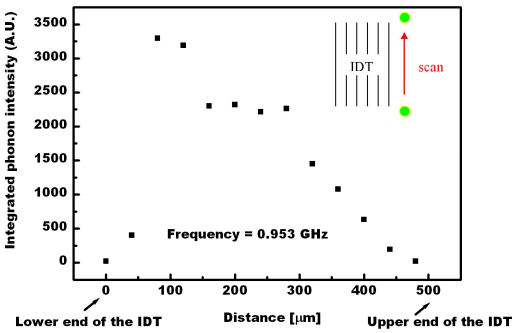

Figure 5 : Induced phonons intensity versus the distance, direction perpendicular to the acoustic beam.

Figure 5 shows the induced phonon amplitude versus the displacement perpendicularly to the acoustic beam. As can be seen the width of the beam is very closed from the aperture of the IDTs. That confirms the good directivity of the induced acoustic wave with a very weak divergence [19]. This result is of great importance because the directivity determines the acoustic coupling efficiency between the emitter and the receiver in a band pass filter application for example.

IV. CONCLUSION

The spatial distribution intensity of the induced phonons has been characterized for surface as well as bulk waves. We can then determine propagation losses of the deposited material

and so find better deposition parameters to reduce these losses in term of acoustic properties that is not so easy with usual X-ray or TEM characterization. We can also give a precise idea of the directivity of our devices in order to enhance the coupling efficiency between emitter and receiver in oscillators, band-pass filters or sensors applications.

We actually work on other materials such as aluminum nitride thin films fabricated by our group in the "Laboratoire de Physique des Milieux Ionisés et Applications".

ACKNOWLEDGMENT

The authors gratefully acknowledge the 'Region Lorraine' and the 'Ministère Français de la Recherche et de la Technologie' for their confidence and the financial support of this work. The authors also wish to acknowledge J.-F. Pautex for his helpful contribution.

REFERENCES

[1] Bömmel H. E. and Dransfeld K. Phys.Rev. **117** 1245
[2] De Klerk J., International Summer School Enrico Fermi (LXIII Corso) p. 437
[3] Monchalin J.-P., 1985, Appl. Phys. Lett. **47** 14
[4] Hesjedal T. and Behme G., 2001, IEEE Trans. Ultrason. Ferroelectrics Frequency Control **48**
[5] Whatmore R. W., Goddard P. A., Tanner B. K. 1982 Proc. Symp. On Ultrasonics
[6] Roschupkin D. V. and Brunel M., 1984 IEEE Trans. Ultrasonics Ferroelectrics Frequency Control **41** 512
[7] Krüger J. K., Embs J., Brierley J., Jimenez, J. Phys. D-Appl. Phys. 31 : 1913 (1998)
[8] Hrüger J. K., Marx A., Peetz L., Roberts R., Unruh H.-G., Colloid & Polymer Sci., 264 : 403-414 (1986)
[9] IRE Standards on Piezoelectric Crystals 1957 Proc. IRE **45** 354.
[10] IRE Standards on Piezoelectric Crystals 1961 Proc. IRE **49** 1161.
[11] Martin S. J., Gunshor R. L., Pierret R. F., Appl. Phys. Lett. 37 (8), 700, (1980)
[12] Hickerwell F. S., IEEE Trans. Son. Ultrason., 32, (5), 621, (1985)
[13] Vellekoop M., Visser C., Sarro P., Venema A., Compatibility of Zinc Oxide with silicon IC processing, Sensors and Actuators, A21-A23 (1990), pp 1027-1030
[14] Krupanidhi S. B., Sayer M., J. Appl. Phys. 56 (11), 3308, (1984)
[15] Hashimoto Ken-ya, "Surface Acoustic Wave Devices in Telecommunication : Modelling and Simulation". Springer, Berlin (2000) p. 242.
[16] Bloch P. D., Doe N. G., Paige E. G. S., Yamaguchi M., Proc. Ultrasonics Symp., IEEE, (1981) 268-273
[17] Grace M. I., Kedzir R. W., Kestigan M., Smith A. B., Appl. Phys. Lett. 9, pp. 155-156 (1966)
[18] Shikata S., Nakahata H., Hachigo, Fujimori N., Diam. Relat. Mater., 2, 1197-1202 (1993)
[19] Krüger J. K., Vincent B., Elmazria O., Bouvot L., Alnot P., New Journal of Physics, 6 : 54 (2004)